An Anisotropic Fourth-Order Partial Differential Equation for Noise Removal

Mohammad Reza Hajiaboli

Department of Electrical and Computer Engineering
Concordia University, Montreal, Canada
mohammad.hajiaboli@ieee.org

Abstract. Fourth-order nonlinear diffusion filters are isotropic filters in which the strength of diffusion at regions with strong image features such as regions with an edge or texture is reduced leading to their preservation. However, the optimal choice of parameter in the numerical solver of these filters for having a minimal distortion of the image features results in a very slow convergence rate and formation of speckle noise on the denoised image especially when the noise level is moderately high. In this paper, a new fourth-order nonlinear diffusion filter is introduced, which have an anisotropic behavior on the image features. In the proposed filter, it is shown that a suitable design of a set of diffusivity functions to unevenly control the diffusion on the directions of level set and gradient leads to a fast convergent filter with a good edge preservation capability. The comparison of the results obtained by the proposed filter with that of the classical and recently developed techniques shows that the proposed method produces a noticeable improvement in the quality of denoised images evaluated subjectively and quantitatively as well as a substantial increment of the convergence rate comparing to the classical filter.

1 Introduction

Nonlinear diffusion denoising filters are known for their good edge preservation capabilities. In these techniques, the denoised image is a solution of a partial differential equation (PDE). The first kind of these denoising methods is introduced by Perona and Malik [1] in 1990 based on solving a nonlinear second-order PDE (i.e. the so-called Perona-Malik equation). Since then, there has been a great deal of research in this filed which led to introduction of variety of nonlinear diffusion denoising techniques (see [2], [3] as a few examples).

In spite of the good edge preservation obtained by these techniques, these methods tend to produce blocky effects in the images [4]. In fact, the solution of Perona-Malik equation is a piecewise constant solution, therefore these filters create blocky effects on the smooth regions of the image. A spatially regularized version of the nonlinear diffusion filter has been introduced by Catte et al. [2] to reduce the formation of the these artifacts on the denoised image. You and Kaveh [4] proposed a more effective solution to this problem by using a fourth-order PDE for noise removal, where a planar approximation of the noisy image

X.-C. Tai et al. (Eds.): SSVM 2009, LNCS 5567, pp. 356–367, 2009.
© Springer-Verlag Berlin Heidelberg 2009

is supported in the solution of the PDE resulting in a significant improvement of the ramp edge preservation and a dramatic reduction of blocky effects. Based on this idea a variety of the fourth-order PDE based denoising techniques have been developed such as the filters given in [5], [6], and [7]. However, the fourth-order diffusion filters damp high spatial frequency components (i.e. noise and step edges) much faster than the second-order ones [5]. This feature can result in distorting of the step edges during the evolutionary process of the image denoising especially when smoothing strength of the filter for the detected edges is not effectively reduced by a diffusivity function. Setting a small threshold value in the diffusivity function substantially reduces the diffusivity on the edges with the expense of a very slow convergence rate, as reported in [4] and [5].

All of previously mentioned techniques belong to a class of diffusion-based denoising filters known as isotropic nonlinear diffusion denoising methods. It means that total amount of the diffusion controlled by the diffusivity function is applied on the different regions of the image regardless of the direction of the image features. To improve edge preservation of these filters, the other class of diffusion-based denoising techniques have been emerged in which the diffusion is adapted to the direction of the local image features [8], [9] and [10]. It means that the filter minimizes the diffusion strength on the direction perpendicular to the direction of local features and maximizes it in the direction of the local features. However, these techniques have been developed in the context of the second-order diffusion filters.

In this paper, an anisotropic fourth-order diffusion filter is proposed in which the diffusion strength is adjusted respecting the direction of the local features. Two different diffusivity functions are designed to extremely minimize the diffusion perpendicular to the feature orientation, while allowing the diffusion parallel to the edge orientation and on the smooth regions to proceed with normal strength. The comparison of the results obtained by the proposed filter with that of the classical and newly developed ones reveals a noticeable improvement in the quality of the denoised images evaluated subjectively and quantitatively as well as a substantial increment of the convergence rate comparing to the classical filter.

2 A Brief Review

2.1 From Second to Fourth-Order Filters

The nonlinear diffusion filters are evolutionary processes. The fundamental PDE of the nonlinear diffusion filter introduced by Perona and Malik [1] is given by

$$\partial u / \partial t = div. \left(c \left(\| \nabla u \| \right) \nabla u \right) \ , \tag{1}$$

where u is the image intensity function, $c(.)$ is a diffusivity function by which the diffusion coefficient is calculated and t is the evolution time. Symbols of $div.$ and $\|.\|$ are used for mathematical notation of Euclidean norm and divergence respectively. The diffusivity function is a positive and none increasing function of $\|\nabla u\|$. One of these diffusivity functions defined by Perona and Malik is given by

$$c\left(\|\nabla u\|\right)=k^{2}/\left(k^{2}+\|\nabla u\|^{2}\right)\ , \tag{2}$$

where k is the so-called contrast parameter.

You and his colleagues [11], carried out a detailed analysis to show that the solution of (1) is equal to the minimization of an energy functional. If the diffusivity function of (2) is used then the energy functional is

$$R\left(u\right)=\int_{\Omega}\frac{k^{2}}{2}\ln\left(k^{2}+\|\nabla u\|^{2}\right)dxdy\ , \tag{3}$$

where Ω is the region of support of u. $R\left(u\right)$ is minimized when $\|\nabla u\|^{2}$ is minimum, which leads to a piecewise constant approximation of u. Therefore, formation of staircase artifacts on the ramp edges is unavoidable. In order to resolve this problem, You and Kaveh [4] introduced a fourth-order PDE-based denoising method in which the denoised image is obtained by minimization of the potential function given by

$$E\left(u\right)=\int_{\Omega}f\left(|\nabla^{2}u|\right)dxdy\ , \tag{4}$$

where $f'\left(s\right)=sc\left(s\right)$and $|\nabla^{2}u|$ is the absolute value of Laplacian of u. Therefore, for the same diffusivity function in (2), *E(u)* is in form of

$$E\left(u\right)=\int_{\Omega}\frac{k^{2}}{2}\ln\left(k^{2}+|\nabla^{2}u|\right)dxdy\ , \tag{5}$$

meaning that *E(u)* is minimized when $|\nabla^{2}u|$ is minimum. Therefore, the ramp region of u (i.e. the regions where $|\nabla^{2}u|=0$) are fit in the solution of the associated fourth-order PDE. The solution of the Minimization problem of (4) after using Euler equation followed by gradient descent procedure is given by

$$\partial u/\partial t=-\nabla^{2}\left(c\left(|\nabla^{2}u|\right)\nabla^{2}u\right)\ , \tag{6}$$

By the forward Euler approximation of the $\partial u/\partial t$, the numerical solver of (6) is given by

$$\begin{aligned}u^{n+1}&=u^{n}-dt\times\nabla^{2}\left(c\left(|\nabla^{2}u^{n}|\right)\nabla^{2}u^{n}\right)\ ,\\ u^{0}&=u_{0}\quad\text{and}\quad n=0,1,\cdots,N\ ,\end{aligned} \tag{7}$$

where n is the number of iterations, dt is the time step-size and u_0 is a noisy image. This process is an iterative process. In order to protect the edges from over-smoothing, the process needs to be ceased at a certain number of iterations denoted by *N*.

Besides these nonlinear diffusion filters, another class of techniques known as regularization techniques based on solving the nonlinear PDE has been widely used for image restoration. The classical paper of Rudin, Osher and Fatemi [12] is introduced one of the first kind of these filters in which PDE to be solved is of the second order. Therefore, the same problem of formation of staircases on the ramp regions of the image motivates the researchers to introduce the new regularization techniques by solving the higher order PDE such as [13], [14]. However, the focus of this paper is on the diffusion based techniques as they have been reviewed earlier.

2.2 Edge Preservation and Convergence Rate

Apart from a significant advancement in reduction of the blocky effects on the denoised image using (6), the optimal parameter setting for numerical solver in (7) leads to very slow convergence rate in its numerical solver especially when the level of contaminating noise is moderately high.

A recently developed technique known as a fourth-order hybrid model [6] uses a relaxed median filter [15] to improve the quality of the denoised image when the observed image is heavily contaminated by noise. The numerical model of this filter is given by

$$u^{n+1} = RM_{\alpha\omega}\left(u^n - dt \times \nabla^2\left(c\left(|\nabla^2 u^n|\right)\nabla^2 u^n\right)\right) \ , \tag{8}$$

where RM denotes the relaxed median filter with a lower bound of α and upper bound of ω. This filtering process needs a lower number of iterations to give a denoised image. However, the denoised image is highly affected by using the relaxed median filter and the main advantage of using fourth-order diffusion filters (i.e. the ramp edge preservation) is hindered as it is shown later. Moreover, the computational burden per iteration is dramatically higher than that of the You and kaveh. Another recently introduced technique [7] demonstrates a significant improvement in the convergence rate along with a good ramp edge preservation. In this technique, the diffusivity function of the You and Kaveh filter, $c\left(|\nabla^2 u|\right)$, is replaced by $c\left(\|\nabla u\|\right)$ and the PDE of the filter is given by

$$\partial u/\partial t = -\nabla^2\left(c\left(\|\nabla u\|\right)\nabla^2 u\right) \ , \tag{9}$$

Although the energy functional of (9) does not have a closed form, it can be seen that the filter can still support the planar approximation of the image. The ramp edge preservation of this fourth-order diffusion filter comes from the fact that $\partial u/\partial t \to 0$ when $\nabla^2 u \to 0$. However, as$|\nabla^2 u| \geq \|\nabla u\|$ the diffusivity function of $c\left(|\nabla^2 u|\right)$ gives the smaller diffusion coefficient for the step edges compared to $c\left(\|\nabla u\|\right)$. Therefore, in spite of the good convergence rate obtained by (9), the step edges are still facing the higher amount of the distortion comparing to that of the classical methods.

2.3 Anisotropic Diffusion Filters

The so-called anisotropic diffusion filters refer to the schemes in which the diffusion rate is specifically controlled based on the direction of the local features such as the ones introduced in [8], [9] and [10]. The coherence-enhancing diffusion filter [9] is one this kind in which the scalar diffusion coefficient in (1) is replaced by a tensor diffusion coefficient to reduce the diffusivity of the filter in perpendicular to the orientation of the local features, while let the diffusion with high strength is performed at the direction of the level set. Another anisotropic filter introduced by Carmona and Zhong [10] uses the scalar diffusivity functions to perform anisotropic diffusion. The PDE of this filter is given by

$$\partial u/\partial t = c_1 \left(c_2 u_{\eta\eta} + c_3 u_{\xi\xi} \right) \ , \tag{10}$$

where c_1,c_2 and c_3 are different diffusivity functions and $u_{\eta\eta}$ and $u_{\xi\xi}$ are the second-order directional derivative. Let η denote the perpendicular direction to the orientation of the feature or the so-called gradient direction and ξ denote the direction of the contour or level set.

All of these techniques belong to a class of filters known as the second-order diffusion filters. Some techniques such as [16] for surface smoothing by anisotropic diffusion filtering of the normals to the surface or its other variant for image denoising [17] can be considered as fourth-order anisotropic filters, however these filters are two phase filters meaning that at the first phase, an anisotropic filter applies on the normal map of the surface or image and at the second phase, a surface is fitted to the processed normals. In Section 3, a new setting of the fourth-order anisotropic diffusion filter is proposed, which is a single phase filter and can be seen as a generalization of the classical fourth-order nonlinear diffusion filter of You and Kaveh.

3 The Proposed Model

3.1 Diffusion Equation

The previously mentioned fourth-order diffusion filters are isotropic in which the extent of the diffusion is controlled by the diffusivity function regardless of the orientation of the edges. The only anisotropic behavior of those filters is limited to the anisotropic response of the discrete Laplacian operator. Most of the discrete Laplacian operators exhibit an anisotropic response to the edge with respect to x and y (i.e. the Cartesian coordination) [18]. However, in order to give an anisotropic realization of the fourth-order diffusion filter, one should consider the second-order directional derivative of the image. Two normalized and orthogonal vectors of η and ξ pointing at the direction of the gradient and level set respectively are given by

$$\eta = \frac{[u_x \ \ u_y]}{\sqrt{u_x^2 + u_y^2}} \ \text{ and } \ \xi = \frac{[-u_y \ \ u_x]}{\sqrt{u_x^2 + u_y^2}} \ . \tag{11}$$

Based on the definition in (11) , one can derive the second order derivative of the image in the direction of the gradient and level set as

$$u_{\eta\eta} = \frac{u_{xx}u_x^2 + 2u_x u_y u_{xy} + u_{yy}u_y^2}{u_x^2 + u_y^2} \tag{12}$$

and

$$u_{\xi\xi} = \frac{u_{xx}u_y^2 - 2u_x u_y u_{xy} + u_{yy}u_x^2}{u_x^2 + u_y^2} \ . \tag{13}$$

However, it can be simply shown that the summation of these second directional derivatives is equal to the Laplacian of the image,

$$\nabla^2 u = u_{xx} + u_{yy} = u_{\xi\xi} + u_{\eta\eta} \ . \tag{14}$$

Therefore, the proposed fourth-order diffusion equation, which is of a generalization of (6) can be written as

$$\partial u/\partial t = -\nabla^2 \left(c_1 \left(c_2 u_{\eta\eta} + c_3 u_{\xi\xi}\right)\right) \ . \tag{15}$$

In the proposed model, c_1, c_2 and c_3 are the diffusivity functions, where c_1 controls total amount of diffusion and c_2 and c_3 control the uneven diffusion in the direction of η and ξ . Apparently, choosing $c_2 = c_3$ and $c_1 * c_2 = c$ will lead to the nonlinear diffusion filter of (6) or (9) depending on the definition of c. In the next section, the criteria of a suitable choice for these diffusivity functions are discussed.

3.2 Diffusivity Functions

Different diffusivity functions in context of nonlinear diffusion denoising have been introduced and depending on the choice of the diffusivity function, the behavior of the filter can be varied. The most commonly used diffusivity function in fourth-order diffusion filters is the one in (2) as $c(s)$, where s is the modulus of the derivative of the image ($s = |\nabla^2 u|$ in (6) or $s = \|\nabla u\|$ in (9). This diffusivity function regardless of the choice of s is a function bounded in (0,1]. However, a low computational cost and suitable choice of these diffusivity functions in our proposed model is given by

$$c_1(s) = c_2(s) = c\left(\|\nabla u\|\right) \ \text{ and } \ c_3 = 1 \ . \tag{16}$$

Similar to (9), s in the function c_1 is the modulus of the gradient of u which leads to a fast convergence rate and $c_2 = c_1$ is an optimal choice in terms of overall computational cost of the filter. Therefore, the proposed model in (15) can be rewritten in the form of

$$\partial u/\partial t = -\nabla^2 \left(\left(c\left(\|\nabla u\|\right)^2 u_{\eta\eta} + c\left(\|\nabla u\|\right) u_{\xi\xi}\right)\right) \ . \tag{17}$$

Since the function c is bounded in $(0, 1]$, the overall diffusivity in η direction is smaller than the one in ξ direction. Before presenting comparative results in the next section, the performance of the filter is compared to the second order filter of Perona Malik in Fig.1, which can show the ability of the proposed filter to preserve the ramp edges. In fact, the proposed filter supports the planar approximation of the image similar to (6) and (9), since for planar regions, $u_{\eta\eta} \to 0$ and $u_{\xi\xi} \to 0$ which lead to $\partial u/\partial t \to 0$.

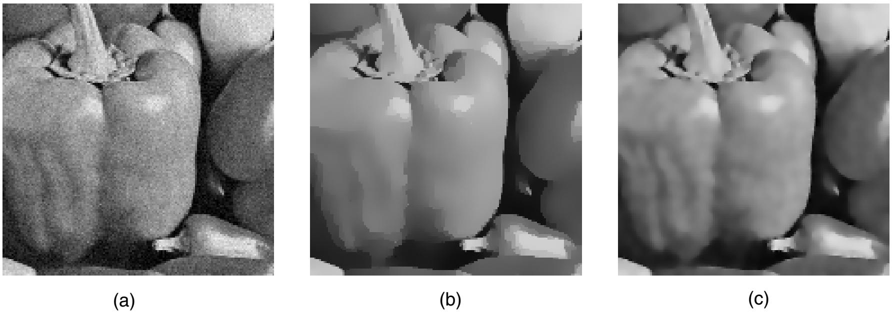

Fig. 1. Comparing the results obtained by a second-order filter and the proposed filter, (a) noisy image, (b) denoised image by the Perona and Malik filter, (c) denoised image by the proposed filter

3.3 Inverse Diffusion

The classical fourth-order filter of You and Kaveh [4] in (6) is a well-posed process because its potential function, (5), is a positive potential function with a global minimum. On the other hand, deriving the potential function of the proposed filter, (17), is not as simple as (6). However, in order to demonstrate that the uneven weighed summation of $u_{\eta\eta}$ and $u_{\xi\xi}$ may lead to the inverse diffusion, it is sufficient to show that at least for a sub-region of u

$$sing\left(c\left(\|\nabla u\|\right)^2 u_{\eta\eta} + c\left(\|\nabla u\|\right) u_{\xi\xi}\right) \neq sign\left(\nabla^2 u\right). \tag{18}$$

In this case, the dynamic flow of (17) performs an inverse diffusion, which results in the edge enhancement.

The maximum of the uneven weight between coefficients of $u_{\eta\eta}$ and $u_{\xi\xi}$ happens, when $c\left(\|\nabla u\|\right) = 1/2$. In this case, the linear version of the (17) can be written in the form of

$$\begin{aligned} \partial u/\partial t &= -\nabla^2\left(\frac{u_{\eta\eta}}{4} + \frac{u_{\xi\xi}}{2}\right) \\ &= -\nabla^2\left(\left(\frac{u_{\eta\eta}}{4} + \frac{u_{\xi\xi}}{4}\right) + \frac{u_{\xi\xi}}{4}\right) \\ &= -\nabla^2\left(\frac{\nabla^2 u}{4} + \frac{u_{\xi\xi}}{4}\right). \end{aligned} \tag{19}$$

Knowing that (6) has a positive potential function, if $sign\left(\nabla^2 u/4 + u_{\xi\xi}/4\right) = sign\left(\nabla^2 u\right)$, it results in a positive potential function for filter (19). It means that $|\nabla^2 u| > |u_{\xi\xi}|$ should be valid throughout the whole image, which does not hold true. An example shown in Fig.2 can demonstrate the fact that the linear diffusion equation of (19) performs an inverse diffusion on the edges. The signal shown in Fig.2-(b) is the extracted intensity profile of the standard test image of *"disk"* in Fig.2-(a) at the middle row. The signal in Fig.2-(c) is the same intensity

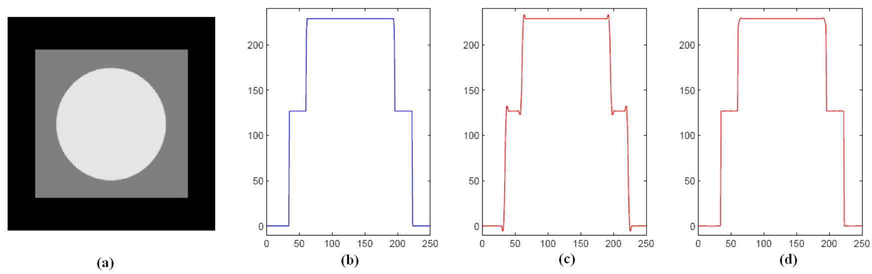

Fig. 2. Inverse diffusion as a result of the uneven diffusion in the directions of η and ξ, (a) is the original image of *"disk"*, (b),(c) and (d) are the intensity of the original, diffused image by (19) and diffused image by the proposed filter (17) at the middle row

profile of the image after being filtered by (19). The inverse diffusion in this case leads to the edge enhancement. However, if the filter is run on the nonlinear fashion as it is proposed in (17), the image shown in Fig.2-(d) shows that process of uplifting of the edges is dramatically reduced. In the other word, in the general application of the image denoising, the process of the inverse diffusion in the proposed filter does not lead to instability of the filter and formation of ringing artifacts around the edges.

4 Comparative Results

In this section, we are presenting the comparative results of the proposed method with the other fourth-order nonlinear diffusion filters. The results of the following filters are going to be compared:

1. The Proposed filter with the PDE of (17) with k=*7* and dt=*0.031* (i.e. the time-step size that provides a data independent stability in the numerical solver [7]).
2. The filter of (7) introduced by You and Kaveh [4] with the suggested parameters setting of dt=*0.25* and k=*1*.
3. The filter of (8) introduced in [12] with the suggested parameters setting of dt=*0.1*, k=*3*, $\alpha = 3$ and $\omega = 5$.
4. The filter in (9) introduced in [7] that is a self-governing filter. In this filter, the diffusivity function of Pernoa and Malik, $c(s)$ has been used with $s = \|\nabla u\|$, the contrast parameter of k is estimated by histogram-based mechanism used in [1] and dt=*0.031*.

Three test images of *"Pepper"*, *"Cameraman"* and *"House"* have been corrupted by white additive Gaussian noise with standard deviation of 15. In Table 1, an objective comparison between the performances of these filters in terms of signal-to-noise ratio (SNR) of the denoised image and their computational complexity are presented.

Table 1. Quantitative comparison of the results

Noisy Image SNR(dB)	Method	Denoised Image SNR(dB)	Num. of Iter.	CPU/Iter.	Convergence(s)
	Proposed	17.84	80	0.038	3.04
Pepper	(9)	17.32	14	0.080	1.12
10.98	(7)	15.83	3133	0.031	97.12
	(8)	15.21	2	0.155	0.31
	Proposed	17.08	35	0.038	1.33
Cameraman	(9)	16.83	6	0.082	0.492
12.38	(7)	16.59	3015	0.031	93.46
	(8)	13.59	1	0.160	0.16
	Proposed	17.44	89	0.038	3.382
House	(9)	17.08	36	0.081	2.916
9.68	(7)	15.80	3907	0.031	121.12
	(8)	15.39	2	0.160	0.32

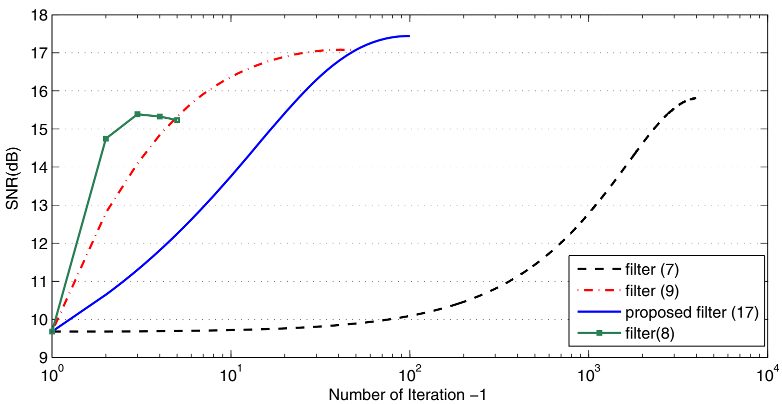

Fig. 3. Comparing the convergence rate of the filters for denoising of test image *"House"*

The results exhibit that the proposed method constantly produces the denoised image with higher SNR. It is important to note that the results are obtained at the optimal number of iterations in which the maximum SNR in evolutionary process of the filters are achieved. If the iterative filtering process is continued after the optimal number of iterations, the SNR of the denoised image is reduced due to over-smoothness of edges.

The other important feature in the proposed method is its fast convergence rate. As it is shown in Fig.3, for the test image of *"House"*, the convergence rate in the proposed method is much higher than the filter of You and Kaveh. The computational burden of the filters is measured as CPU time of each iteration provided that they are filtering the same image on the same computer. Thus, the total convergence time for filtering process is a multiplication of CPU/iteration by number of iterations. The relaxed median regularized filter converges faster

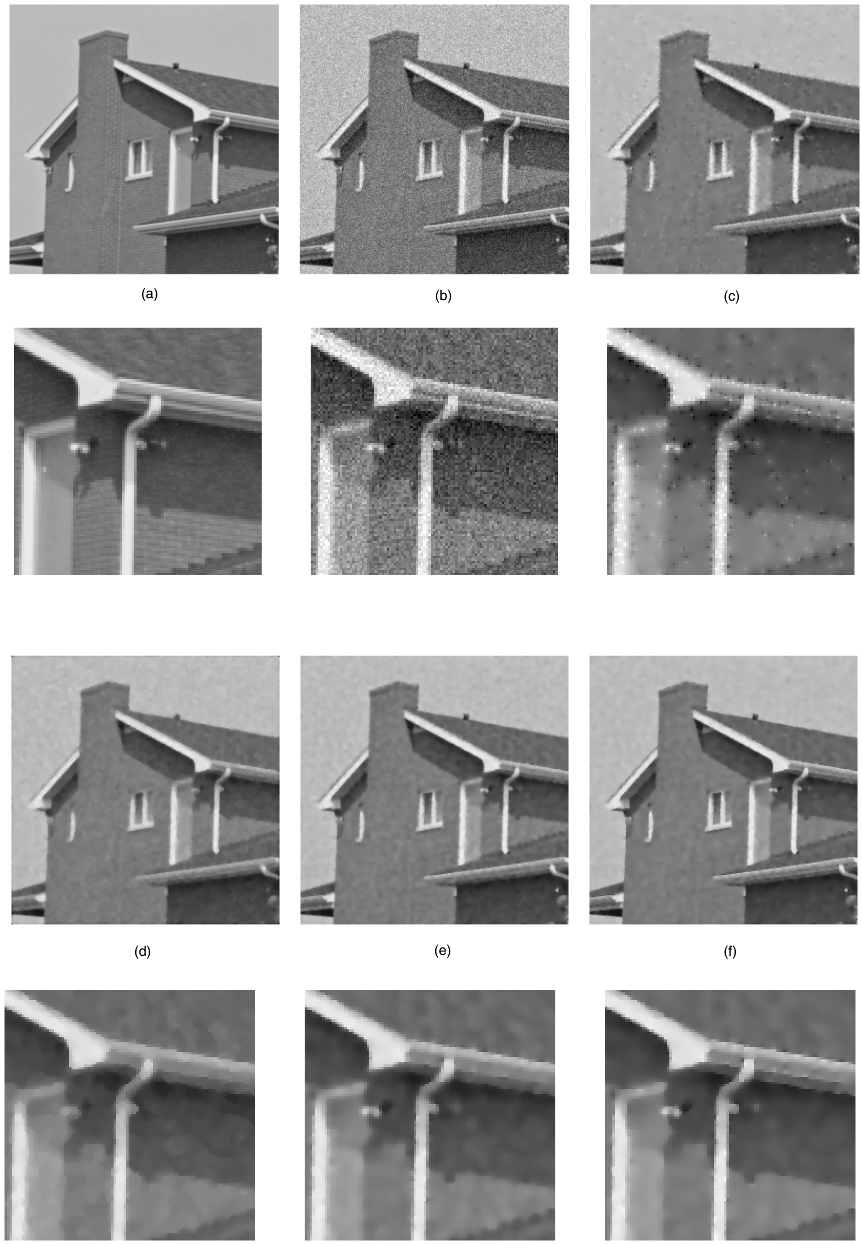

Fig. 4. Comparing the perceptual quality of the results. The pair of images labeled (a) to (f) are as the following: (a) noiseless image, (b) noisy image, (c) denoised image using (7), (d) denoised image using (8), (e) denoised image using (9), (f) is denoised image using proposed filter (17).

than the proposed method, however the maximum SNR is significantly lower than that of other methods, and the decay rate of SNR due to over-smoothness of the edges is also very fast. The computational cost of the proposed filter compared to the one in (9) is slightly higher, however the higher SNR obtained by the proposed filter justifies this amount of the higher computational burden.

In Fig.4, the perceptual quality of the denoised image by the proposed method is compared with that of the other methods. In the first row, the whole image and in the second row, a magnified portion of the image are shown. Each pair of the images is labeled from (a)-(f). The first two images (a) and (b) are the noiseless and the noisy images. In Fig.4-(c), the denoised image by You and Kaveh filter is shown in which formation of some speckle noise on the denoised image is visible. This drawback is known and addressed in [4] and it is as a result of choosing small value for k in diffusivity function, however this setting of k is necessary to protect the edges from over-smoothing. In Fig.4-(d), the denoised image by the relaxed median regularized filter using (8) is shown. This denoised image is blurred and some staircase artifacts on smooth regions of the image are formed. The next image, shown in Fig.4-(e) is the result of the filter in (9) in which the extent of denoising and edge preservation is noticeably better than that of the filters of (7) and (8). However, comparing this result with the one obtained by the proposed filter in Fig. 4-(f) reveals that the extent of edge preservation in the proposed filter is noticeably higher.

5 Conclusion

An anisotropic fourth-order PDE for noise removal has been proposed. A brief theoretical review of the second and fourth-order diffusion denoising filters has been presented with highlighting the fact that previously developed fourth-order filters are isotropic filters in which the extent of the edge preservation is controlled by reduction of the diffusivity of the filters near the edge regardless of its orientation. A major challenge in these filters is that the optimal choice of the model parameters for good edge preservation leads to a dramatically slow convergence rate. However, in the proposed filter, the diffusion strength has been adjusted with respect to the direction of the local features. Two different diffusivity functions have been designed to extremely minimize the diffusion in perpendicular to the feature orientation (i.e. gradient direction), while let the diffusion on the direction parallel to the orientation of the edge (i.e. direction of the level set) proceed with normal speed. Therefore, the proposed filter leads to a faster reduction of the uncorrelated noise and overall faster convergence rate with a good edge preservation due to reduction of the diffusivity of the filter in the gradient direction. The comparison of the results obtained by the proposed filter with that of the classical and newly developed ones has shown that the proposed method produces a noticeable improvement in the quality of the denoised images evaluated subjectively and quantitatively as well as a substantial increment of the convergence rate compared to the classical filter.

References

1. Perona, P., Malik, J.: Scale-space and edge detection using anisotropic diffusion. IEEE Trans. on Pattern Analysis and Machine Intelligence 12(7), 629–639 (1990)
2. Catte, F., et al.: Image selective smoothing and edge detection by nonlinear diffusion. SIAM J. Numer. Anal. 29(1), 182–193 (1992)
3. Black, M.J., et al.: Robust anisotropic diffusion. IEEE Transactions on Image Processing 7(3), 421–432 (1998)
4. You, Y.L., Kaveh, M.: Fourth-order partial differential equations for noise removal. IEEE Transactions on Image Processing 9(10), 1723–1730 (2000)
5. Lysaker, M., Lundervold, A., Tai, X.-C.: Noise removal using fourth-order partial differential equation with applications to medical magnetic resonance images in space and time. IEEE Tran. on Image Processing 12(12), 1579–1590 (2003)
6. Rajan, J., Kannan, K., Kaimal, M.R.: An Improved hybrid model for molecular image denoising. Journal of Mathematical Imaging and Vision 31, 73–79 (2008)
7. Hajiaboli, M.R.: A self-governing hybrid model for noise removal. In: Wada, T., Huang, F., Lin, S. (eds.) PSIVT 2009. LNCS, vol. 5414, pp. 295–305. Springer, Heidelberg (2009)
8. Weickert, J.: Anisotropic Diffusion in Image Processing. B. G. Teubner (1998)
9. Weickert, J.: Coherence-enhancing diffusion filtering. International Journal of Computer Vision 31(2-3), 111–127 (1998)
10. Carmona, R.A., Zhong, S.: Adaptive smoothing respecting feature directions. IEEE Transactions on Image Processing 7(3), 353–358 (1998)
11. You, Y.-L., et al.: Behavioral analysis of anisotropic diffusion in image processing. IEEE Trans. Image Processing 5, 1539–1553 (1996)
12. Rudin, L., Osher, S., Fatemi, E.: Nonlinear Total Variation based noise removal algorithms. Physica D 60, 259–268 (1992)
13. Chan, T., Marquina, A., Mulet, R.: High Order Total Variation-based Image Restoration. SIAM J. on Scientific Computing 22(2), 503–516 (2000)
14. Fang, L., et al.: Image restoration combining a total variational filter and a fourth-order filter. Journal of Visual Communication and Image Representation 18(4), 322–330 (2007)
15. Hamza, A.B., et al.: Removing noise and preserving details with relaxed median filters. Journal of Mathematical Imaging and Vision 11(2), 161–177 (1999)
16. Tasdizen, T., et al.: Geometric surface smoothing via anisotropic diffusion of normals. IEEE visualization 1(1), 125–132 (2002)
17. Lysaker, M., Osher, S., Tai, X.-C.: Noise removal using smoothed normals and surface fitting. IEEE Transactions on Image Processing 13(10), 1345–1357 (2004)
18. Kamgar-Parsi, B., Rosenfeld, A.: Optimally isotropic Laplacian operator. IEEE Transactions on Image Processing 8(10), 1467–1472 (1999)